NONUNIFORM LINEAR ANTENNA ARRAYS FOR ENHANCED NEAR FIELD SOURCE LOCALIZATION

Houcem Gazzah

Dept. of Elec. and Computer Engineering
University of Sharjah, 27272, UAE
hgazzah@sharjah.ac.ae

Jean Pierre Delmas

Telecom SudParis, UMR CNRS 5157
91011 Evry, France
jean-pierre.delmas@it-sudparis.eu

ABSTRACT

Arrays of sensors freely located along an axis are considered in this paper that are used to localize a near-field emitting source. Using Taylor expansion and a suitable coordinate system, simple, yet rich to interpret, Cramer-Rao bounds relative to the direction and range parameters are derived. Our analysis allows in particular to unveil a family of non-uniform linear arrays with better near field estimation capabilities, compared to the well-established uniform linear arrays.

Index Terms— Direction of arrival, range, near-field, antenna arrays, performance analysis, Cramer-Rao bound.

1. INTRODUCTION

Antenna arrays is a major field of statistical signal processing and direction finding is among the most investigated topics [1]. The complexity of the antenna array near-field propagation model explains the limited research and the scarcity of results, the existing literature being mostly concerned with antenna arrays far-field analysis and applications. A recent interest in parameter estimation of near-field sources has just emerged, focusing on the Cramer-Rao Bounds (CRB) of DOA and range estimated by means of the Uniform Linear Array (ULA) [2, 3] and the Uniform Circular Array (UCA) [4], respectively. Despite the importance and wide use of the ULA and the UCA, these results are of limited interest, especially if one thinks about the developing interest about irregular array geometries and methods to design advantageous (w.r.t. the ULA) non-uniform linear arrays [5]. This paper addresses linear arrays with freely spaced sensors and shows that there is a room to outperform the ULA from the viewpoint of near-field source localization.

Our Taylor expansion of the CRB is based on the exact time delay formula, similarly as [2, 3], but uses a different coordinate system. It judiciously leads to more compact and more interpretable CRB expressions that apply to arbitrary linear arrays. For instance, we identify a class of *centro-symmetric* linear arrays with better near-field estimation capabilities. They include, but are not limited to, the ULA. In fact, within centro-symmetric linear arrays, we identify some geometric parameters that characterize linear (but non-uniform) arrays with better estimation than the ULA for near-field sources, while being equivalent for far-field sources.

The paper is organized as follows. Sec. 2 presents the near-field signal model and coordinate system. Sec. 3 is dedicated to the derivation of simple and interpretable closed-form expressions of the CRB on DOA and range. Then, Sec. 4 is focused on the special class of centro-symmetric arrays and key-geometric parameters that determine their performance. This ultimately leads to non-uniform centro-symmetric arrays that achieve better accuracy than the ULA for localizing near-field sources. A conclusion is given is Sec. 5.

2. SIGNAL MODEL

We consider a linear antenna array of P sensors $C_1, \cdots, C_P$ located along the x-axis, at coordinates $x_1, \cdots, x_P$, respectively, as shown on Fig. 1. The array centroid is assumed to be at the origin O, which allows for a more compact expressions of the CRB, compared to [2, 6]. A source S emits a narrow-band signal $s(t)$ (with wavelength λ) in the direction of the antenna array. It is at a distance r from the origin O and forms an angle θ with $[O, y)$. At time t, the source originates at sensor p the snapshot $y_p(t) = \exp(i\tau_p)\, s(t) + n_p(t)$, where $n_p(t)$ represents the ambient additive noise, while $\tau_p \hat{=} 2\pi(SO - SC_p)/\lambda$ is also equal to

$$\tau_p = 2\pi \frac{r}{\lambda}\left(1 - \sqrt{\beta_p}\right), \quad \text{with } \beta_p \hat{=} 1 - 2\frac{x_p}{r}\sin(\theta) + \frac{x_p^2}{r^2}.$$

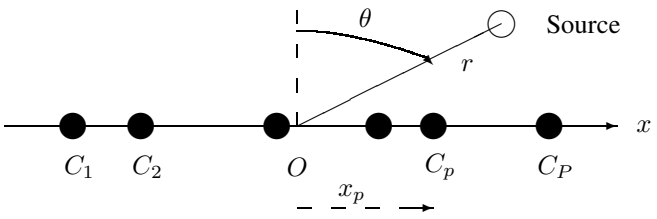

Fig. 1. Source in the near-field of the arbitrary linear array.

978-1-4799-2893-4/14/$31.00 ©2014 IEEE

Based on N snapshots $\{y_p(t)\}_{p=1,...,P;t=t_1,...,t_N}$, estimates of both range r and DOA θ are obtained using a variety of algorithms. Some are capable of achieving the CRB [7]. Indeed, we adopt the stochastic CRB as our evaluation criterion, assuming the usual statistical properties about $n_p(t)$ and $s(t)$: (i) $n_p(t)$ and $s(t)$ are independent, (ii) $\{n_p(t)\}_{p=1,...,P;t=t_1,...,t_N}$ are independent, zero-mean circular Gaussian distributed with variance σ_n^2, (iii) $\{s(t)\}_{t=t_1,...,t_N}$ are assumed to be independent zero-mean circular Gaussian distributed with variance σ_s^2 (the so-called unconditional or stochastic model).

3. TAYLOR EXPANSION OF THE CRB

To derive the stochastic CRB on θ and r, we use the general matrix expression of the stochastic CRB given for several parameters per source [8] and adapted to a single source. This gives $\mathbf{CRB}(\theta,r)=\mathbf{F}^{-1}$ with

$$\mathbf{F}=\frac{2N\sigma_s^4}{\sigma_n^2(\sigma_n^2+P\sigma_s^2)}\left[P\mathbf{D}^H\mathbf{D}-\mathbf{D}^H\mathbf{a}\mathbf{a}^H\mathbf{D}\right], \quad (1)$$

where $\mathbf{a}=[e^{i\tau_1},...,e^{i\tau_P}]^T$ is the steering vector and $\mathbf{D}$ the derivative $[\frac{\partial\mathbf{a}}{\partial\theta},\frac{\partial\mathbf{a}}{\partial r}]$. A long proof (proofs can be found in [9]) leads to the following expression of the 2×2 matrix $\mathbf{F}$:

$$\begin{aligned}
\frac{2c}{r\cos^3(\theta)}[\mathbf{F}]_{1,2} &= P\frac{S_3}{r^3}+\sin(\theta)\frac{3PS_4-S_2^2}{r^4}+o(\epsilon^4)\\
\frac{c}{r^2\cos^2(\theta)}[\mathbf{F}]_{1,1} &= P\frac{S_2}{r^2}+2P\sin(\theta)\frac{S_3}{r^3}\\
&\quad+\frac{S_4P\left[4\sin^2(\theta)-1\right]-S_2^2\sin^2(\theta)}{r^4}+o(\epsilon^4)\\
\frac{c}{\cos^4(\theta)}[\mathbf{F}]_{2,2} &= \frac{1}{4}\frac{PS_4-S_2^2}{r^4}+\frac{PS_5-S_2S_3}{r^5}\sin(\theta)\\
&\quad+\frac{PS_6\left[23\sin^2(\theta)-3\right]-3S_2S_4\left[5\sin^2(\theta)-1\right]+8S_3^2\sin^2(\theta)}{8r^6}+o(\epsilon^6)
\end{aligned}$$

where $S_k\hat{=}\sum_{p=1}^P x_p^k$ (with in particular, $S_1=0$) are purely geometric, $c\hat{=}\frac{\lambda^2}{4\pi^2}\frac{\sigma_n^2(\sigma_n^2+P\sigma_s^2)}{2N\sigma_s^4}$, $\epsilon\hat{=}\frac{1}{r}\max_p|x_p|$ and $o(\epsilon^k)$ satisfying $\lim_{\epsilon\to 0}o(\epsilon^k)/\epsilon^k=0$.

From $[\mathbf{F}]_{1,2}$, the DOA is decoupled from the range to the second-order in ϵ iff $S_3=0$. This class of arrays that will be studied in details in Sec. 4 will have many advantages. For the moment, we give results for arbitrary values of S_3.

From the above, the following expressions of the CRB on the DOA and range are obtained after tedious derivations.

$$\begin{aligned}
\mathrm{CRB}(\theta) &= \frac{c}{P}\frac{1}{S_2-\frac{PS_3^2}{PS_4-S_2^2}}\frac{1+\gamma_1\frac{\sin(\theta)}{r}}{\cos^2(\theta)}+o(\epsilon) \quad (2)\\
\frac{\mathrm{CRB}(r)}{r^4} &= \frac{4c}{PS_4-S_2^2-P\frac{S_3^2}{S_2}}\frac{1+\gamma_2\frac{\sin(\theta)}{r}}{\cos^4(\theta)}+o(\epsilon) \quad (3)
\end{aligned}$$

where $\gamma_1\hat{=}4PS_3\frac{S_2S_3^2-S_2^2S_4+PS_4^2-PS_3S_5}{(PS_4-S_2^2)(PS_2S_4-S_2^3-PS_3^2)}$ and $\gamma_2\hat{=}2\frac{3PS_2S_3S_4+S_2^3S_3-PS_3^3-2PS_2^2S_5}{S_2(PS_2S_4-S_2^3-PS_3^2)}$.

In these CRB expressions, terms in $1/r$ vanish if $S_3=0$ in (2) and if $S_3=S_5=0$ in (3). This is not a marginal scenario as it concerns in particular the ULA. To cover these cases, we prove that, for arrays with $S_3=0$, we have

$$\mathrm{CRB}(\theta)=c\frac{1+\left[1+\left(1+\frac{4PS_4}{PS_4-S_2^2}\right)\sin^2(\theta)\right]\frac{S_4}{S_2}\frac{1}{r^2}}{\cos^2(\theta)PS_2}+o(\epsilon^2). \quad (4)$$

For those satisfying both $S_3=0$ and $S_5=0$, we have

$$\frac{\mathrm{CRB}(r)}{r^4}=\frac{4c}{\cos^4(\theta)}\frac{1+\frac{\gamma_3(\theta)}{2(PS_4-S_2^2)r^2}}{PS_4-S_2^2}+o(\epsilon^2) \quad (5)$$

where $\gamma_3(\theta)\hat{=}\frac{18P^2S_4^2+2S_2^4+3PS_2^2S_4-23P^2S_2S_6}{PS_2}\sin^2(\theta)+3PS_6-3S_2S_4$.

4. CENTRO-SYMMETRIC ARRAYS

We define centro-symmetric arrays as those linear arrays with sensors disposed symmetrically w.r.t. the origin, ones with coordinates of the form $\pm x^{(1)},\pm x^{(2)},\cdots$, with, possibly, a sensor at the origin. Obviously, such an array verifies $S_i=0$ for any odd i. The opposite is not always true. Actually we prove that[1] an array is centro-symmetric iff $S_i=0$ for any odd i less or equal to P. We will rather focus on the closed-form expressions (4)-(5) to analyze the impact of the array geometry (in terms of the non-zero S_2, S_4 and S_6) on the array estimation performance for both DOA and range, of both far-field and near-field sources.

4.1. Relations between far-field and near-field DOA performance

We start by recalling the stochastic DOA CRB in the far-field propagation model [11, rel. (5)] given for arbitrary linear arrays by

$$\mathrm{CRB}_{\mathrm{FF}}(\theta)=\frac{c}{\cos^2(\theta)PS_2}. \quad (6)$$

Compared to (4), we realize that arrays for which $S_3=0$ (including centro-symmetric arrays) achieve $\mathrm{CRB}_{\mathrm{FF}}(\theta)$ when the source-to-array distance tends to infinity. At the same time, θ and r estimates are decoupled, as pointed out earlier. Other advantages of centro-symmetric arrays include a larger domain of validity of our approximations as a result of the convergence in $1/r^2$ compared to $1/r$ for non centro-symmetric arrays. More unusual is the behavior of non centro-symmetric arrays (and, in general, those with a non-zero S_3). Because [1] $PS_4-S_2^2>0$, such arrays verify

$$\lim_{r\to\infty}\mathrm{CRB}(\theta)>\mathrm{CRB}_{\mathrm{FF}}(\theta).$$

[1] Proofs, detailed in [9], about S_2, S_4 and S_6 are based on the Newton-Girard Formula [10, pp. 69-74] that allows iterative calculation of S_i.

Now, w.r.t. $[\mathbf{F}]_{1,2}$, θ and r are coupled to the second-order in ϵ. More precisely, the square of $[\mathbf{F}]_{1,2}$ and the term $[\mathbf{F}]_{2,2}$ tend to zero with the same speed. This is in contrast to the case $S_3 = 0$, for which the square of $[\mathbf{F}]_{1,2}$ tends to zero more rapidly than $[\mathbf{F}]_{2,2}$ when r tends to ∞. Consequently, from the practical point-of-view, as far as only the DOA parameter is considered, the far-field propagation model, although approximative, may be preferable to the exact near-field model for non centro-symmetric arrays with $S_3 \neq 0$.

To illustrate the different behavior of centro-symmetric and non centro-symmetric arrays in the near-field region, we test in Fig. 2 antenna arrays of $P = 4$ sensors. On the one hand, the ULA with a constant inter-sensors spacing d and for which $S_3 = S_5 = 0$. On the other hand, the minimum hole and redundancy linear array (MHRLA) with inter-spacings d, $3d$, $2d$ [12] and for which $S_3 \neq 0$. Thanks to a larger aperture, the MHRLA exhibits a lower far-field CRB, for instance, $\mathrm{CRB}_{\mathrm{FF}}^{\mathrm{MHRLA}}(\theta)/\mathrm{CRB}_{\mathrm{FF}}^{\mathrm{ULA}}(\theta) \approx 0.22$. However, due to the coupling of θ and r in the the matrix $\mathbf{F}$ of the MHRLA, we have $\lim_{r\to\infty} \mathrm{CRB}(\theta) > \mathrm{CRB}_{\mathrm{FF}}(\theta)$ for this array. Furthermore, this figure confirms that the domain of validity of our approximations is much larger for the centro-symmetric than for non centro-symmetric arrays.

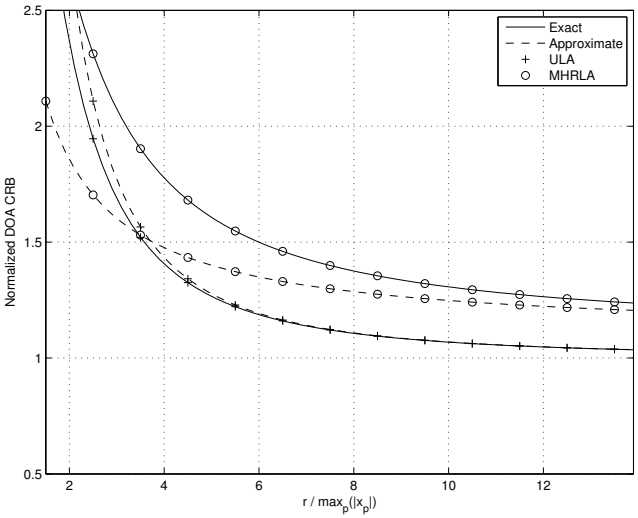

Fig. 2. Approximative [(from (2), (4))] and exact [deduced from (1)] ratios $\mathrm{CRB}(\theta)/\mathrm{CRB}_{\mathrm{FF}}(\theta)$ for 4-sensors ULA and MHRLA and a source at $\theta = 50°$.

4.2. Near-field performance

We have favored centro-symmetric arrays verifying $S_3 = 0$ mainly because they do not suffer degradation in the DOA CRB when source tends to be in the antenna far-field. Among those arrays with $S_3 = 0$, those with identical S_2 achieve the same far-field DOA CRB. Now, out from these ones, we will be able to identify better ones, on the basis of the DOA and range (near-field) CRBs. The following rewriting of (4-5) will be helpful for this purpose

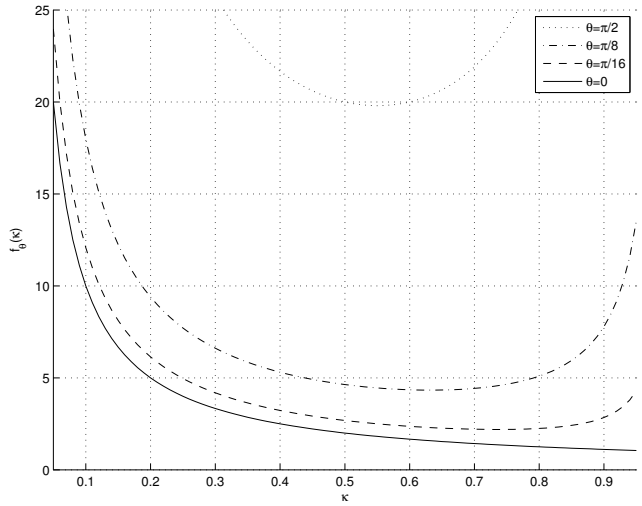

Fig. 3. Near-field DOA estimation performance, as expressed by $f_\theta(\kappa)$, as function of the geometry of the centro-symmetric array, as expressed by parameter κ.

$$\mathrm{CRB}(\theta) = c\frac{\frac{1}{S_2} + \frac{1}{\kappa}\left[\left(1+\frac{4}{1-\kappa}\right)\sin^2(\theta)+1\right]\frac{1}{Pr^2}}{\cos^2(\theta)P} + o(\epsilon^2) \quad (7)$$

$$\frac{\mathrm{CRB}(r)}{r^4} = c\frac{1}{\cos^4(\theta)}\frac{4}{S_2^2}\left[\frac{1}{\frac{1}{\kappa}-1} + \frac{S_2}{2Pr^2} \times \frac{\left(18+3\kappa+2\kappa^2-\frac{23}{\eta}\right)\sin^2(\theta)+3\frac{\kappa^2}{\eta}-3\kappa}{(1-\kappa)^2}\right] + o(\epsilon^2). \quad (8)$$

where

$$\kappa \hat{=} \frac{S_2^2}{PS_4} \quad \text{and} \quad \eta \hat{=} \frac{S_2^3}{P^2 S_6}$$

appear as two key geometric parameters that determine the near-field accuracy of the antenna array. They also can be proved to verify the following interesting properties [1]

$$\eta \leq \kappa \leq 1$$

and

$$\eta \simeq \frac{4}{5\left(\frac{3}{\kappa}-\frac{5}{2}\right)} \text{ for } P \gg 1.$$

While S_2 determines the array far-field DOA estimation performance, κ and η are all what matters for near-field DOA and range estimation performance. In practice, only κ is important, in regard of the predominant terms in (7) and (8). It affects (8) through the increasing function $1/(1/\kappa - 1)$, and affects (7) through function $f_\theta(\kappa)$

$$f_\theta(\kappa) \hat{=} \frac{1}{\kappa}\left[\left(1+\frac{4}{1-\kappa}\right)\sin^2(\theta)+1\right],$$

illustrated in Fig. 3. Considering DOA estimation, choosing κ loosely close to $1/2$ ensures limited degradation in all look directions. If κ is close to (but lower than) $1/2$, then it also ensures better estimation of the range parameter as well.

4.3. Comparison with the ULA

To better illustrate the impact of κ on the estimation performance of both DOA and range, we compare the 6-sensors ULA (with sensors placed at ± 0.1195, ± 0.3586 and ± 0.5976) against a non-ULA array of 6 sensors located at ± 0.1281, ± 0.2396 and ± 0.6528. Both arrays exhibit the same $S_2 = 1$ (and, hence, have identical far-field DOA estimation CRBs). However, κ is equal to 0.577 for the ULA and to 0.45 for the non-ULA.

In Fig. 4, we report the ratios

$$\frac{\mathrm{CRB}(\theta)|_{\mathrm{non-ULA}}}{\mathrm{CRB}(\theta)|_{\mathrm{ULA}}} \text{ and } \frac{\mathrm{CRB}(r)|_{\mathrm{non-ULA}}}{\mathrm{CRB}(r)|_{\mathrm{ULA}}},$$

calculated using the exact CRB expressions and the approximate CRB expressions in (7) and (8). There, we can see that while we obtain similar DOA performance (with a slight degradation), the non-ULA array has better range estimation capabilities. From (7), all centro-symmetric linear arrays characterized by a given size P and a given value of S_2 verify

$$\lim_{r\to\infty} \frac{\mathrm{CRB}(\theta)|_{\mathrm{non-ULA}}}{\mathrm{CRB}(\theta)|_{\mathrm{ULA}}} = 1.$$

However, from (8), the κ-dependent function

$$\mathcal{R}_P(\kappa) \doteq \lim_{r\to\infty} \frac{\mathrm{CRB}(r)|_{\mathrm{non-ULA}}}{\mathrm{CRB}(r)|_{\mathrm{ULA}}} = \frac{\frac{1}{\kappa_{\mathrm{ULA}}} - 1}{\frac{1}{\kappa} - 1}$$

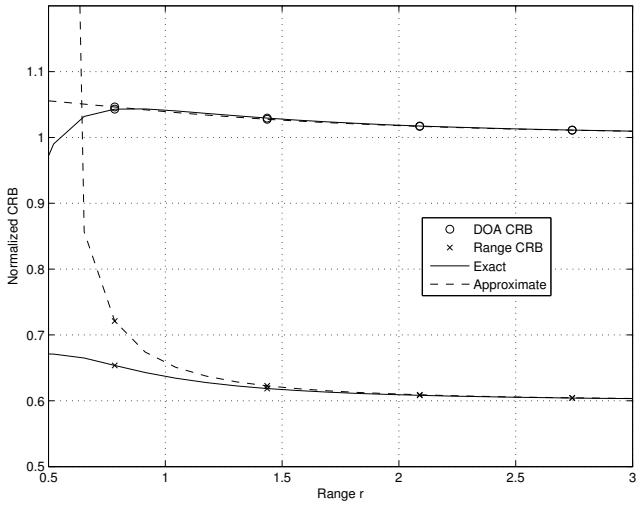

Fig. 4. DOA and range CRBs of the non-ULA ($\kappa = 0.45$) normalized to that of the equivalent ULA ($\kappa = 0.577$) for $\theta = 40°$. Both arrays are made of $P = 6$ sensors and are such that $S_2 = 1$.

can be seen as an indicator of improvement (over the ULA) whenever it is lower than one. For instance, if $P \gg 1$,

$$\mathcal{R}_P(\kappa) = \frac{4}{5}\frac{1}{\frac{1}{\kappa} - 1}.$$

This ratio is illustrated in Fig. 5 for the domain[2] $[0.3, 0.7]$ of κ outside which DOA near-field performance degrades severely (as clear from Fig. 3). It can be seen from Fig. 5 that the (far-field) range CRB can be reduced by a much as 50% by antenna arrays with a κ moderately lower than that of the ULA.

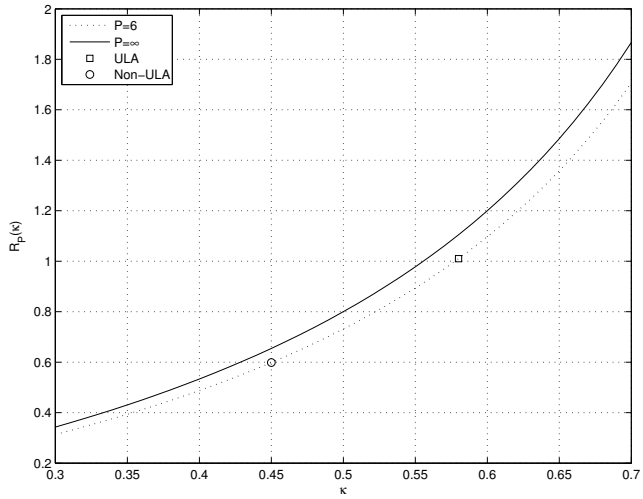

Fig. 5. Centro-symmetric non-ULA versus ULA: Compared range estimation performance of far-field sources.

5. CONCLUSION

Accurate, simple and interpretable closed-form expressions of the CRB for both angle and range parameters of a near-field narrow-band source have been obtained for arbitrary linear arrays using the exact expression of the time delay parameter. They show the exact geometric condition for the antenna array to have an attractive behavior in its near-field: better precision and faster convergence to the far-field DOA CRB. Such a class of centro-symmetric arrays includes, but is not restricted to the ULAs. Furthermore, it is proved that appropriately designed centro-symmetric non-ULA can largely improve the range estimates without deteriorating the DOA estimates under near-field conditions.

[2] In fact, extreme values of κ (i.e., 0 and 1) are achieved by impractically co-localized sensors, either at the origin, or at the same distance (and on both sides) from the origin.

6. REFERENCES

[1] H. Krim and M. Viberg, "Two decades of array signal processing research," *IEEE Signal Process. Mag.*, vol. 13, no. 4, pp. 67-94, Jul. 1996.

[2] Y. Begriche, M. Thameri, and K. Abed-Meraim, "Exact Cramer Rao bound for near field source localization," in *Proc. International Conference on Information Science, Signal Processing and their Applications*, 2012, pp. 718-721.

[3] Y. Begriche, M. Thameri, and K. Abed-Meraim, "Exact conditional and unconditional Cramer Rao bound for near field localization," in arXiv.

[4] J. P. Delmas and H. Gazzah, "CRB Analysis of near-field source localization using uniform circular arrays," in *Proc. ICASSP*, Vancouver pp. 3396-3400, 2013.

[5] M. Rubsamen, A. B. Gershman, "Sparse Array Design for Azimuthal Direction-of-Arrival Estimation," *IEEE Trans. Signal Process.*, vol. 59, no. 12, pp. 5957-5969, Dec. 2011.

[6] M. N. El Korso, R. Boyer, A. Renaux, and S. Marcos, "Conditional and unconditional Cramer Rao bounds for near-field Source localization," *IEEE Trans. Signal Process.*, vol. 58, no. 5, pp. 2901-2906, May 2010.

[7] H. Gazzah and J. P. Delmas, "Spectral efficiency of beamforming-based parameter estimation in the single source case," in *Proc. IEEE SSP*, Nice, pp. 153-156, 2011.

[8] H. Abeida ans J. P. Delmas, "Efficiency of subspace-based DOA estimators," *Signal Processing*, vol. 87, no. 9, pp. 2075-2084, Sept. 2007.

[9] H. Gazzah and J. P. Delmas, "CRB based-design of linear antenna arrays for near-field source localization," *IEEE Trans. Antennas Propag.*, accepted.

[10] L. E. Dickson, *Elementary Theory of Equations*, New York, Wiley and Sons, 1914.

[11] C. ElKassis, J. Picheral, and C. Mokbel, "Advantages of nonuniform arrays using root-MUSIC", *Signal Processing*, Elsevier, vol. 90 (210), pp. 689-695.

[12] Y. Meurisse and J. P. Delmas, "Bounds for sparse planar and volume arrays," *IEEE Trans. Inform. Theory*, vol. 47, no. 1, pp. 464-468, January 2001.